Renewable Energy xxx (2014) 1–8

Contents lists available at ScienceDirect

Renewable Energy

journal homepage: www.elsevier.com/locate/renene

A new analytical model for wind-turbine wakes

Majid Bastankhah, Fernando Porté-Agel*

Wind Engineering and Renewable Energy Laboratory (WIRE), École Polytechnique Fédérale de Lausanne (EPFL), EPFL-ENAC-IIE-WIRE, 1015 Lausanne, Switzerland

ARTICLE INFO

Article history:
Received 29 September 2013
Accepted 4 January 2014
Available online xxx

Keywords:
Wind-turbine wakes
Analytical models
Gaussian model
Top-hat model
Velocity deficit

ABSTRACT

A new analytical wake model is proposed and validated to predict the wind velocity distribution downwind of a wind turbine. The model is derived by applying conservation of mass and momentum and assuming a Gaussian distribution for the velocity deficit in the wake. This simple model only requires one parameter to determine the velocity distribution in the wake. The results are compared to high-resolution wind-tunnel measurements and large-eddy simulation (LES) data of miniature wind-turbine wakes, as well as LES data of real-scale wind-turbine wakes. In general, it is found that the velocity deficit in the wake predicted by the proposed analytical model is in good agreement with the experimental and LES data. The results also show that the new model predicts the power extracted by downwind wind turbines more accurately than other common analytical models, some of which are based on less accurate assumptions like considering a top-hat shape for the velocity deficit.

© 2014 Elsevier Ltd. All rights reserved.

1. Introduction

Due to the fast growth in the number and size of installed wind farms around the world, wind-turbine wakes have become important topics of study. As many wind turbines in wind farms have to operate in the wakes of upwind turbines, they are exposed to incoming wind velocities that are smaller than those under unperturbed (unwaked) conditions. As a result, turbine wakes are responsible for important power losses in wind farms [1–3]. Extensive analytical, numerical and experimental efforts have been carried out to better understand and predict turbine wake flows. Although numerical and experimental techniques have become increasingly sophisticated and accurate in recent years, simple analytical models are still useful tools to predict wind-turbine wake flows and their effect on power production. They are widely used due to their simplicity and low computational cost [4]. Various analytical investigations have been conducted on wind-turbine wakes (e.g., [5–7]). One of the pioneering analytical wake models is the one proposed by Jensen [8], which assumes a top-hat shape for the velocity deficit in the wake (see Fig. 1a) and states:

$$\frac{\Delta U}{U_\infty} = \left(1 - \sqrt{1 - C_T}\right) \Big/ \left(1 + \frac{2k_{wake}x}{d_0}\right)^2, \tag{1}$$

where C_T is the thrust coefficient of the turbine, k_{wake} the rate of wake expansion, d_0 the diameter of the wind turbine and x the downwind distance. $\Delta U/U_\infty$ is the normalized velocity deficit, which is defined as:

$$\frac{\Delta U}{U_\infty} = \frac{U_\infty - U_w}{U_\infty}, \tag{2}$$

where U_∞ is the incoming wind velocity and U_w the wake velocity in the streamwise direction. Jensen [8] considered a constant value for the rate of wake expansion ($k_{wake} = 0.1$). However, the suggested values for k_{wake} in the literature are 0.075 [9] for on-shore cases and 0.04 [10,11] or 0.05 [9,12] for off-shore ones. Katić et al. [5] also used the top-hat model proposed by Jensen [8]. They claimed that the top-hat model gives an estimate of the energy content rather than describing the velocity field accurately, and hence they adopted a top-hat shape for the velocity deficit in the wake because of its simplicity and low computational cost. Nevertheless, note that the energy available in the wind varies as the cube of the wind speed [13] and, therefore, an improper evaluation of velocity field in a wind farm can lead to large errors in the prediction of the energy output. This will be discussed in detail in Section 3.

Eq. (1) has been extensively used in the literature (e.g., Marmidis et al. [14]) and commercial softwares such as WAsP [9], WindPRO [15], WindSim [16], WindFarmer [17] and OpenWind [18]. However, there are two important limitations of this simple model that should be pointed out: (a) The assumption of the top-hat distribution of the velocity deficit is not realistic [19,20]. (b) Even though

* Corresponding author. EPFL-ENAC-IIE-WIRE, Bâtiment GR, Station 2, 1015 Lausanne, Switzerland. Tel.: +41 21 6932726.
E-mail address: fernando.porte-agel@epfl.ch (F. Porté-Agel).

0960-1481/$ – see front matter © 2014 Elsevier Ltd. All rights reserved.
http://dx.doi.org/10.1016/j.renene.2014.01.002

Please cite this article in press as: Bastankhah M, Porté-Agel F, A new analytical model for wind-turbine wakes, Renewable Energy (2014), http://dx.doi.org/10.1016/j.renene.2014.01.002

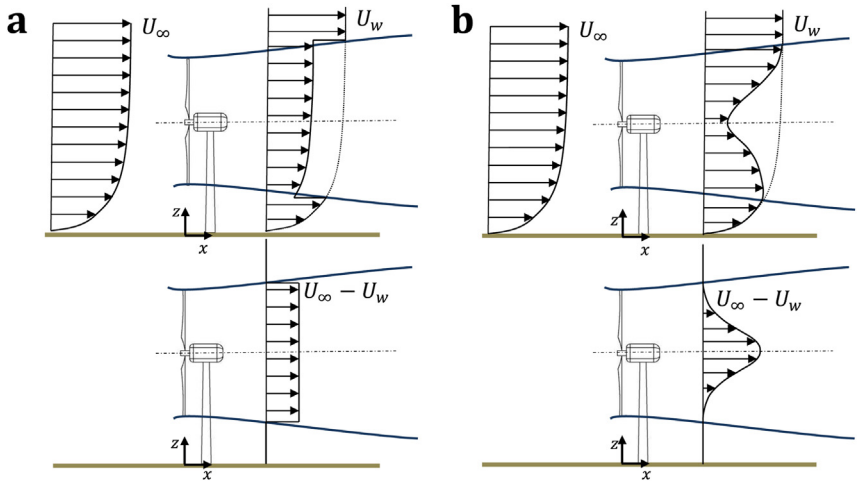

Fig. 1. Schematic of the vertical profiles of the mean velocity (top) and velocity deficit (bottom) downwind of a wind turbine obtained by assuming: (a) a top-hat and (b) a Gaussian distribution for the velocity deficit in the wake.

Jensen [8] and Katić et al. [5] claimed using momentum conservation to derive Eq. (1), it will be shown in the following that in reality they only used mass conservation to derive their model.

Jensen [8] considered a control volume immediately downwind of the turbine. Fig. 2a shows a schematic of this control volume with the left cross-sectional area (side 1) equal to the area swept by the wind-turbine blades, A_0, and the right area (side 3) equal to the cross-sectional area of the wake, A_w. The incoming flow also enters into the control volume through the lateral surface (side 2) with the velocity of U_∞. According to mass conservation:

$$\dot{m}_2 = \rho U_w A_w - \rho U_a A_0, \tag{3}$$

where $\dot{m}_2$ is the mass flow rate through the lateral surface, ρ the density of the air and U_a the wind velocity just behind the wind turbine (see Fig. 2a). Note that if $\dot{m}_2$ is replaced with $\rho U_\infty (A_w - A_0)$ in the mass conservation equation (Eq. (3)), without considering momentum conservation, the basic equation that Jensen [8] used to establish his model will be obtained. It implies, therefore, that this model can be derived by considering mass conservation alone without any consideration of the balance of momentum.

Later, Frandsen et al. [21] applied mass and momentum conservation to a control volume around the turbine (Fig. 2b) and proposed the following expression for the velocity deficit in the wake:

$$\frac{\Delta U}{U_\infty} = \frac{1}{2}\left(1 - \sqrt{1 - 2\frac{A_0}{A_w}C_T}\right), \tag{4}$$

where $A_w(x=0) = A_a$, and A_a is the cross-sectional area of the wake just after the initial wake expansion. In other words, they assumed that the distance downwind of a rotor that the flow requires to reach the pressure of the free flow is negligible, so they considered A_a as the wake cross-sectional area at $x = 0$. It is, however, difficult to identify exactly this distance in reality. Crespo et al. [4] stated that the length of this region is in the order of one rotor diameter. Even though this assumption is crude, it ensures a solution for all C_T values between 0 and 1 [21]. According to the actuator disk concept [13], A_a is given by:

$$A_a = \beta A_0, \tag{5}$$

where β is a function of C_T and can be expressed as:

$$\beta = \frac{1}{2}\frac{1 + \sqrt{1 - C_T}}{\sqrt{1 - C_T}}. \tag{6}$$

They also used an asymptotic solution for an infinite row of two-dimensional obstacles to write the wake diameter, d_w, as:

$$d_w = (\beta + \alpha x/d_0)^{1/2} d_0, \tag{7}$$

where the expansion factor α is of order 10 k_{wake} [21]. While Frandsen et al. [21] employed the mass and momentum equations, their model still assumed a top-hat shape for the velocity deficit in the wake.

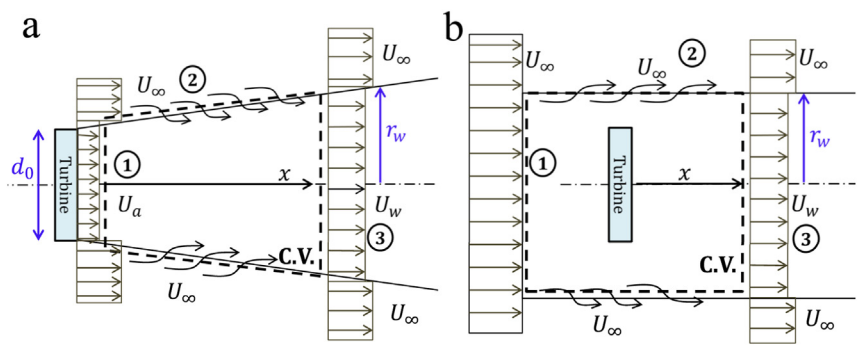

Fig. 2. Schematic of the two control volumes: (a) downwind of the wind turbine, and (b) around the wind turbine.

Please cite this article in press as: Bastankhah M, Porté-Agel F, A new analytical model for wind-turbine wakes, Renewable Energy (2014), http://dx.doi.org/10.1016/j.renene.2014.01.002

Wakes of bluff bodies in free stream flows have been extensively studied in classical theories of shear flows (e.g., [22–24]). In these studies, the self-similar Gaussian profile of the velocity deficit is found in the far-wake regions. For wind-turbine wakes in turbulent boundary layers, even though the velocity distribution does not show axisymmetric behavior [25], the velocity deficit in the wake has an approximately Gaussian axisymmetric shape after some downwind distances [25,26] (Fig. 1b). This Gaussian shape of the velocity deficit in turbine wakes has been observed by wind-tunnel measurements (e.g., [25,27–30]), numerical simulations, (e.g., [31]) and data of operating wind farms (e.g., [20,32]). Therefore, the Gaussian distribution is appropriate to describe the velocity deficit in the far wake regions, regardless of the incoming wind conditions.

The intention of the work described in this paper is to propose and validate a simple and efficient analytical model for the prediction of the velocity downwind of a wind turbine. For this purpose, a Gaussian distribution is considered for velocity deficit profiles in the wake, and momentum and mass conservation are applied to find the velocity distribution downwind of the wind turbine. The results are tested against the wind-tunnel measurements [19] and the LES data [33] for the wake of a miniature wind turbine, as well as the LES data [31] of a real-scale wind turbine under four different atmospheric turbulence conditions.

In Section 2, the wake model is derived. The results are then presented and compared with wind-tunnel measurements and LES data in Section 3. The summary and future research are presented in Section 4.

2. Wake model

If we neglect viscous and pressure terms in the momentum equation, the following equation can be obtained for the wake by applying mass and momentum conservation (see Tennekes and Lumley [22]):

$$\rho \int U_w(U_\infty - U_w)\mathrm{d}A = T, \tag{8}$$

where T is the total force over the wind turbine. T can be determined by (see Burton et al. [13]):

$$T = \frac{1}{2}C_T \rho A_0 U_\infty^2. \tag{9}$$

Next, the self-similarity in the wake describes the normalised velocity deficit as [34]:

$$\frac{\Delta U}{U_\infty} = C(x) f(r/\delta(x)), \tag{10}$$

where $C(x)$ represents the maximum normalized velocity deficit at each downwind location which occurs at the center of the wake; r is the radial distance from the center of the wake and $\delta(x)$ the characteristic wake width at each x. As explained in the previous section, the velocity deficit in the turbine wake, regardless of incoming conditions, is assumed to have a Gaussian shape. Thus, Eq. (10) can be written as:

$$\frac{\Delta U}{U_\infty} = C(x) e^{-\frac{r^2}{2\sigma^2}}, \tag{11}$$

where σ is the standard deviation of the Gaussian-like velocity deficit profiles at each x. Note that σ is not associated with *turbulent velocity fluctuations* in this paper. According to Eq. (11), the wake velocity is given by:

$$U_w = U_\infty \left(1 - C(x) e^{-\frac{r^2}{2\sigma^2}}\right). \tag{12}$$

Inserting Eqs. (9) and (12) into Eq. (8) and integrating from 0 to ∞ yield:

$$8\left(\frac{\sigma}{d_0}\right)^2 C(x)^2 - 16\left(\frac{\sigma}{d_0}\right)^2 C(x) + C_T = 0. \tag{13}$$

By solving Eq. (13), one can obtain two values for $C(x)$ while only one of them, which predicts the smaller value for the velocity deficit at larger downwind distances, is physically acceptable:

$$C(x) = 1 - \sqrt{1 - \frac{C_T}{8(\sigma/d_0)^2}}. \tag{14}$$

If we assume a linear expansion for the wake region like the one considered by Jensen [8], σ/d_0 can be written as:

$$\frac{\sigma}{d_0} = k^* \frac{x}{d_0} + \varepsilon, \tag{15}$$

where $k^* = \partial\sigma/\partial x$ is the growth rate and ε is equivalent to the value of σ/d_0 as x approaches zero. Note that $k^* = \partial\sigma/\partial x$ is different from $k_{wake} = \partial r_w/\partial x$ used by Jensen [8]. Inserting Eqs. (14) and (15) into Eq. (11) and rearranging give:

$$\frac{\Delta U}{U_\infty} = \left(1 - \sqrt{1 - \frac{C_T}{8(k^* x/d_0 + \varepsilon)^2}}\right) \times \exp\left(-\frac{1}{2(k^* x/d_0 + \varepsilon)^2}\left\{\left(\frac{z - z_h}{d_0}\right)^2 + \left(\frac{y}{d_0}\right)^2\right\}\right), \tag{16}$$

where y and z are spanwise and vertical coordinates, respectively, and z_h is the hub height. Eq. (16) gives the normalized velocity deficit in the wake as a function of normalized coordinates (x/d_0, y/d_0 and z/d_0), C_T and k^*. In order to use the above equation, the value of ε should be determined in advance.

Next, the value of ε will be determined by equating the total mass flow deficit rate at $x = 0$ obtained by Frandsen model [21] and the one obtained by the new proposed model (Eq. (16)). The velocity deficit just behind the turbine is usually assumed to have a uniform distribution and it changes to a Gaussian shape further downstream. Thus, at $x = 0$, Eq. (16) is not likely to predict the velocity profile accurately. However, the total mass flow deficit rate at $x = 0$ predicted by this equation should be the same as the one obtained by Frandsen model [21] since both of these models are derived by applying the same governing equations. According to Eq. (4), the total mass flow deficit rate at $x = 0$ obtained by Frandsen model is:

$$\int \frac{\Delta U}{U_\infty}\mathrm{d}A = \frac{\pi}{8} d_0^2 \beta \left(1 - \sqrt{1 - \frac{2}{\beta} C_T}\right), \tag{17}$$

where β is defined in Eq. (6). On the other hand, from Eq. (16), the total mass flow deficit rate at $x = 0$ based on the new proposed model is given by:

Please cite this article in press as: Bastankhah M, Porté-Agel F, A new analytical model for wind-turbine wakes, Renewable Energy (2014), http://dx.doi.org/10.1016/j.renene.2014.01.002

Table 1
Different experimental and LES case studies used to validate the new proposed model.

Cases	$d_0(m)$	$z_h(m)$	$U_{hub}(m/s)$	C_T	$z_0(m)$	$I_0(z = z_h)$
Case 1	0.15	0.125	2.2	0.42	0.00003	0.070
Case 2	80	70	9	0.8	0.5	0.134
Case 3	80	70	9	0.8	0.05	0.094
Case 4	80	70	9	0.8	0.005	0.069
Case 5	80	70	9	0.8	0.00005	0.048

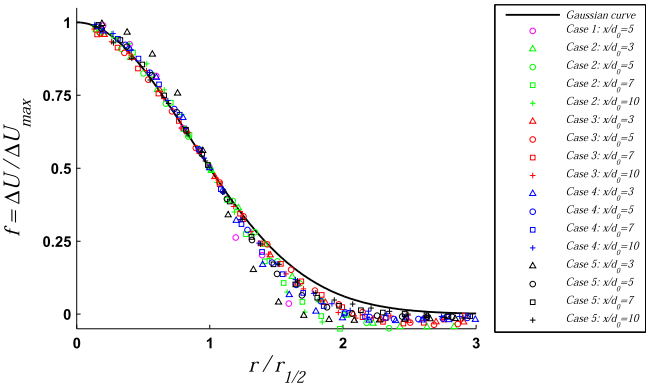

Fig. 3. The self-similar velocity deficit profiles of the wind-tunnel measurements [19] (Case 1) and the LES data [31] (Cases 2–5) at different downwind distances.

$$\int \frac{\Delta U}{U_\infty} dA = \int_0^{+\infty} \left(1 - \sqrt{1 - \frac{C_T}{8\varepsilon^2}}\right) \exp\left(\frac{-r^2}{2\varepsilon^2 d_0^2}\right) 2\pi r dr = 2\pi\varepsilon^2 d_0^2 \left(1 - \sqrt{1 - \frac{C_T}{8\varepsilon^2}}\right). \quad (18)$$

By equating Eqs. (17) and (18), it can be concluded that:

$$\varepsilon = 0.25\sqrt{\beta}. \quad (19)$$

3. Results and discussion

In this section, we present the results obtained by the new proposed model and compare them with 5 different LES and experimental case studies (see Table 1). Case (1) in Table 1 corresponds to the wind-tunnel measurements reported by Chamorro and Porté-Agel [19] and the LES performed by Wu and Porté-Agel [33] to investigate the wake of a miniature wind turbine in a turbulent boundary layer flow. Later, Wu and Porté-Agel [31] also used LES to study the effect of atmospheric turbulence on wakes of real-scale wind turbines. To this end, they simulated the wake of a Vestas V80-2MW wind turbine with four different aerodynamic surface roughness lengths (Cases 2–5 in Table 1). Note that I_0 denotes the ambient streamwise turbulence intensity in Table 1, and z_0 is the aerodynamic roughness of the terrain. These roughness lengths shown for Cases (2–5) in Table 1 are representative of different land surface types, including very rough terrain ($z_0 = 0.5$ m), farmlands ($z_0 = 0.05$ m), grasslands ($z_0 = 0.005$ m), and snow-covered flats ($z_0 = 0.00005$ m) [31].

Fig. 3 shows the self-similar velocity-deficit profiles $f = \Delta U/\Delta U_{max}$ for wind-tunnel measurements [19] (Case 1) and the LES data [31] (Cases 2–5) at different downwind distances. The wake's half-width $r_{1/2}(x)$, defined at each x as

$$\frac{\Delta U\left(r = r_{1/2}\right)}{U_\infty} = \frac{1}{2}\frac{\Delta U_{max}}{U_\infty} = \frac{1}{2}C(x), \quad (20)$$

is used as the characteristic wake width in this figure. The figure shows that the profiles of $f = \Delta U/\Delta U_{max}$ plotted against $r/r_{1/2}$ approximately collapse onto a single Gaussian curve except at the edge of the wake. It means that the velocity deficit profile can be assumed to have a self-similar Gaussian shape after some downwind distance ($x/d_0 \gtrsim 3$).

In Fig. 4, the normalized standard deviation of the Gaussian curves fitted to the velocity deficit profiles in the wakes is plotted as a function of normalized downwind distance for the different cases. It shows that the wake expands approximately linearly in the range of $2 < x/d_0 < 15$ for the different cases, although classical theories of shear flows predict the wake width varies as $x^{1/3}$ [22]. This discrepancy might be due to the following reasons: (1) To derive this power law dependence of wake width on x in classical studies, $\Delta U/U_\infty$ at the wake center is assumed to tend to zero (lower than 0.1) [34] whereas it is not a good assumption in our region of interest ($x/d_0 \lesssim 20$) for the turbine wake (see values of $\Delta U/U_\infty$ in Fig. 5). (2) More importantly, in classical studies (e.g., [22]), the effect of ambient turbulence intensity on the wake growth is not

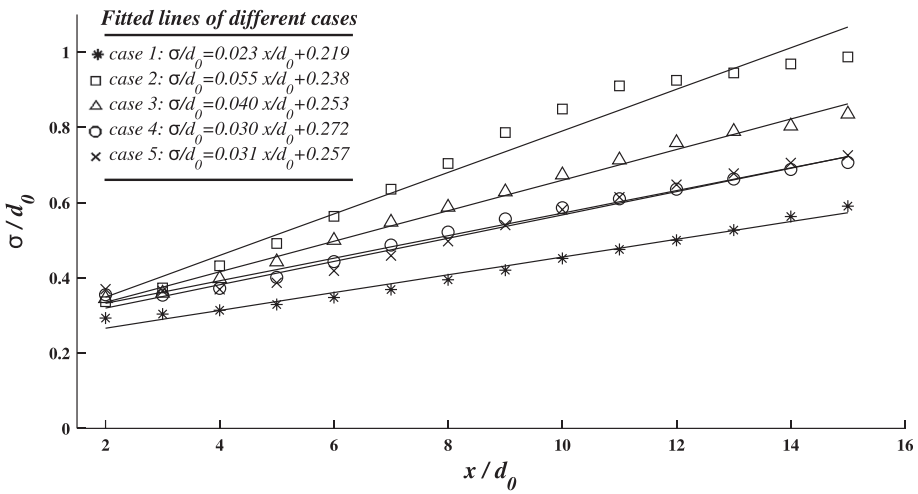

Fig. 4. Normalized standard deviation of the velocity deficit profiles: case 1 (asterisk), case 2 (square), case 3 (triangle), case 4 (circle) and case 5 (crosses). Fitted lines are represented by solid lines.

Please cite this article in press as: Bastankhah M, Porté-Agel F, A new analytical model for wind-turbine wakes, Renewable Energy (2014), http://dx.doi.org/10.1016/j.renene.2014.01.002

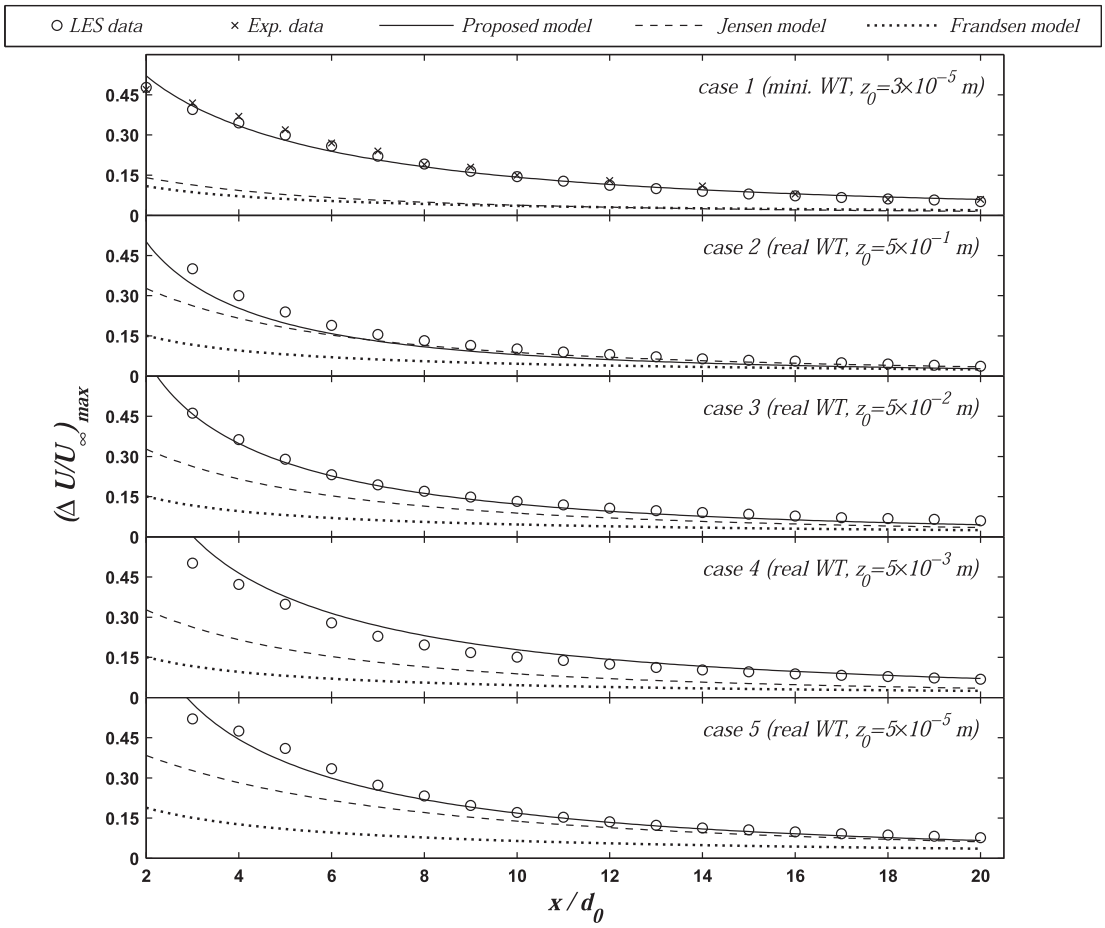

Fig. 5. Normalized velocity deficit, at hub height, versus normalized downwind distance in the wake of wind turbines (Cases 1–5): Wind-tunnel measurements [19] (crosses), LES data [33,31] (open circle), new proposed model (solid line), Jensen model [8] (dashed line) and Frandsen model [21] (dotted line).

considered [4]. In turbulent boundary layers, the wake is, however, known to recover faster than in non-turbulent flows since both ambient turbulence and shear-generated turbulence contribute to the growth rate in this case (e.g., [31]). Thus, it seems reasonable to observe a faster wake recovery compared to that predicted by classical studies.

The figure also shows that the wakes recover faster with increasing the ambient turbulence intensity (compare Cases 2–5). It is due to the fact that higher incoming turbulence enhances mixing processes, which result in faster wake recovery. However, the wake recovery is approximately the same for Cases (4) and (5) with different ambient turbulence intensities. One possible explanation is that the ratio of the ambient turbulence intensity to the turbulence intensity added by turbines is small in Cases (4) and (5). Thus, the wake recovery in these cases is likely to be more influenced by the turbulence added by the turbine than the ambient turbulence. Now, let us compare Case (4) with the higher value of C_T to Case (1) with the lower value of C_T but approximately the same value of I_0. Fig. 4 shows that the wake width in Case (4) is larger than Case (1). However, it seems that this difference is mostly created at smaller downwind distances, and it remains approximately constant further downstream ($x/d > 6$). It is worth mentioning that the above discussions about the wake growth behavior are based on the experimental and numerical results presented in this research. In fact, we believe that deep understanding of the turbine wake growth under different conditions suffers from the lack of fundamental studies, and thus, we aim to extensively study this in our future research.

The value of ε for the different cases can also be estimated by extrapolating the fitted lines in Fig. 4. The comparison between the values of ε obtained by extrapolating the LES data and the ones derived analytically (Eq. (19)) reveals that Eq. (19) is able to predict the trend for the different cases in such a way that the turbines with higher values of C_T (Cases 2–5) generally have larger values of ε compared to the one with lower value of C_T (Case 1). Nonetheless, Eq. (19) overestimates the value of ε for all cases. It is probably due to the fact that we equated the total mass flow rate at $x = 0$ obtained by the new proposed model with the one proposed by Frandsen et al. [21] to derive the value of ε. As discussed in Section 1, Frandsen et al. [21] neglected the distance downwind of the turbine that the flow requires to reach the pressure of the free flow and so assumed that $A_w(x = 0) = A_a$ where A_a is determined by Eq. (5). Hence, in reality the value predicted by Eq. (19) corresponds to some small distance downwind of the turbine, instead of immediately behind the turbine. The value of ε should therefore be lower than the one predicted by Eq. (19). According to the LES data shown in Fig. 4, the below expression with the lower constant coefficient gives a better estimation of the value of ε for the different cases:

$$\varepsilon = 0.2\sqrt{\beta}. \tag{21}$$

In the following, the results obtained by the new proposed and other analytical models are compared against LES and experimental data for the different cases. For the new proposed model, the value of k^* is found from the LES data of the different cases (see Fig. 4), then Eq. (16) is used to predict the velocity deficit in the

Please cite this article in press as: Bastankhah M, Porté-Agel F, A new analytical model for wind-turbine wakes, Renewable Energy (2014), http://dx.doi.org/10.1016/j.renene.2014.01.002

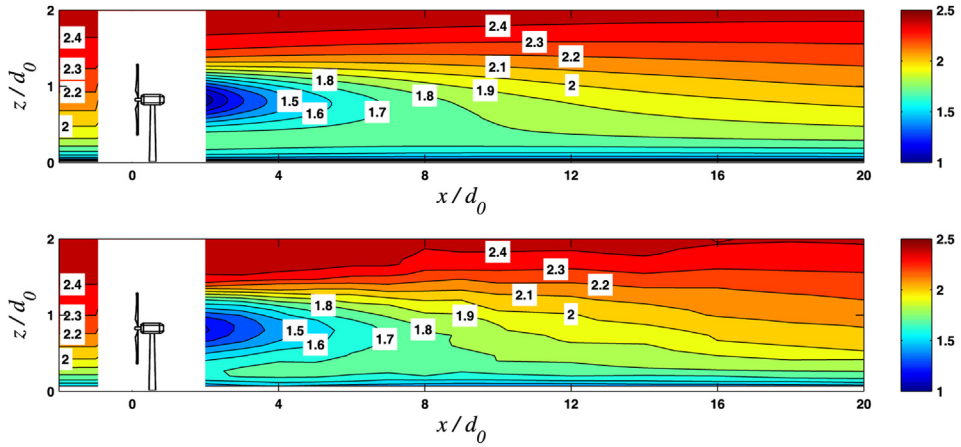

Fig. 6. Contours of streamwise velocity (ms^{-1}) in the vertical plane normal to the wind turbine, at zero span (Case 1): New proposed model (top) and wind-tunnel measurements [19] (bottom).

wake for each case. For Jensen model, k_{wake} is set to 0.05 for Case (5) since the surface roughness in this case is on the order of off-shore cases, and $k_{wake} = 0.075$ is used for other cases. Fig. 5 shows the change of the normalized velocity deficit, at turbine hub height, as a function of normalized downwind distance for different analytical models, the wind-tunnel measurements performed by Chamorro and Porté-Agel [19] and the LES data reported by Wu and Porté-Agel [33] and Wu and Porté-Agel [31]. The figure shows that the model proposed by Jensen [8] can predict the maximum velocity deficit reasonably well in some regions (e.g., $x/d_0 > 6$ in Case 2), but this model underestimates the maximum velocity deficit in other regions with respect to the LES [33,31] and experimental data [19]. This underestimation is more obvious for relatively small downwind distances ($x/d_0 < 8$). This departure can be attributed to: (a)

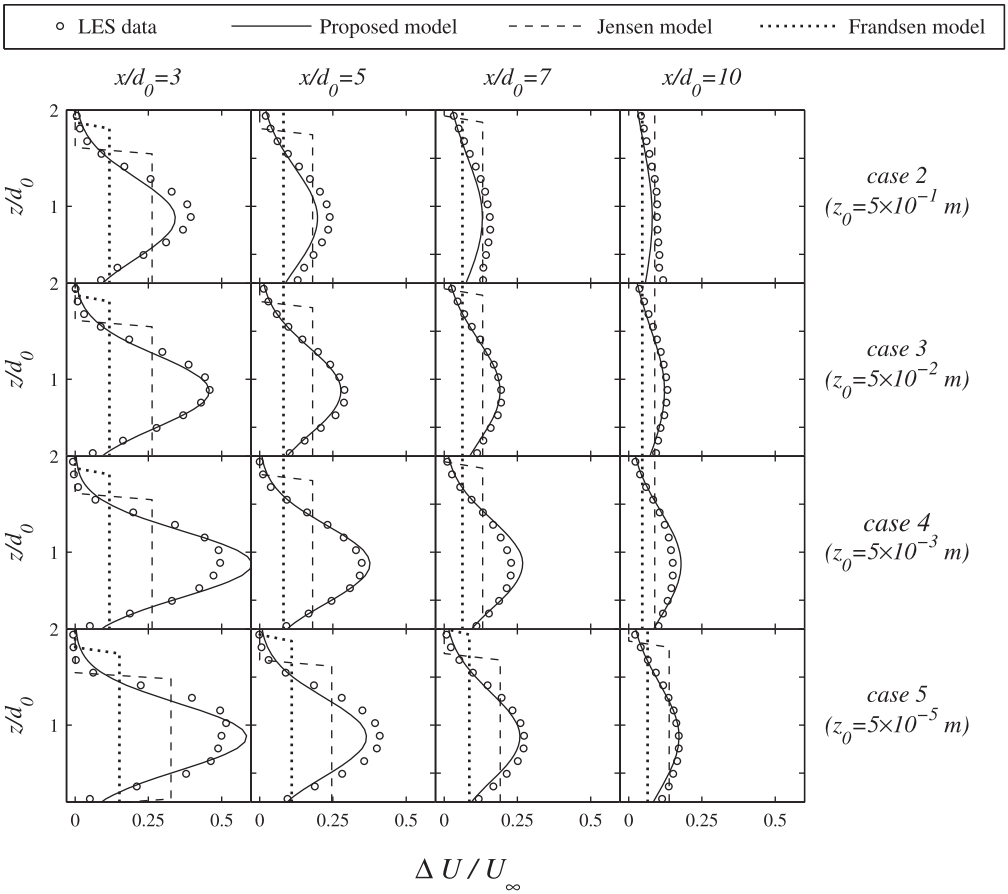

Fig. 7. Vertical profiles of the normalized velocity deficit in the wakes of real-scale turbines installed on flat surfaces with different roughness lengths (Cases 2–5): LES data [31] (open circle), new proposed model (solid line), Jensen model [8] (dashed line) and Frandsen model [21] (dotted line).

Please cite this article in press as: Bastankhah M, Porté-Agel F, A new analytical model for wind-turbine wakes, Renewable Energy (2014), http://dx.doi.org/10.1016/j.renene.2014.01.002

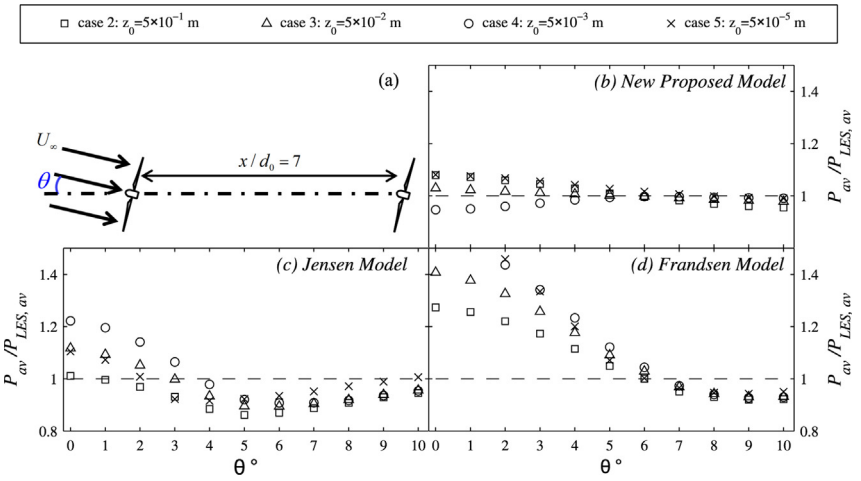

Fig. 8. Variation of $P_{av}/P_{LES,av}$ at $x/d_0 = 7$ as a function of wind direction for different analytical models: Case 2 (square), Case 3 (triangle), Case 4 (circle), and Case 5 (crosses).

the assumption of a uniform velocity distribution in the wake which leads to the observed underestimation at the center of the wake (where the maximum velocity deficit is found), and (b) the sole use of mass conservation to derive the model. The model proposed by Frandsen et al. [21] also underestimates the velocity deficit at turbine hub height. In addition to the top-hat assumption for the velocity deficit, the failure of their model can be attributed to the assumed nonlinear expansion for the wake which is, as described earlier, not in agreement with the LES data at distances $x/d_0 < 20$. On the other hand, the new proposed model is able to predict reasonably well the maximum velocity deficit in the wake of miniature and real-scale wind turbines placed over different land surface types, ranging from a very rough terrain (Case 2) to a smooth one (Case 5). We only need to have a reasonable estimation of the growth rate k^*.

Fig. 6 shows contours of the streamwise velocity for Case (1) measured in the wind-tunnel experiment [19] and predicted by the proposed analytical model on a vertical plane perpendicular to the wind turbine at zero span. It shows that the results obtained with the new proposed model are in acceptable agreement with the wind-tunnel measurements, and the model can thoroughly capture the non-axisymmetric velocity distribution in the wake due to the presence of the turbulent boundary layer.

Vertical profiles of the velocity deficit in Cases (2–5) for the different analytical models and the LES data [31] are shown in Fig. 7 for chosen downwind locations ($x/d = 3,5,7,10$). The figure shows that the results obtained from the proposed model for the velocity deficit in the wake of the real-scale turbine are in acceptable agreement with the LES data [31] at different heights. It also shows that the top-hat models not only do underestimate the velocity deficit at hub height but also overestimate it near the edge of the wake.

It should be mentioned that the effect of ground on turbine wakes is neglected in this research. The ground can generally have two effects on turbulent wake flows: (a) suppression of turbulent velocity near the ground, and (b) the inviscid potential effect of the ground [35]. Firstly, since the suppression of turbulence due to the presence of the ground occurs in a region very close to the ground, its effect is assumed to be trivial at the hub-height level. Secondly, the inviscid potential effect can be simulated by imaging techniques. Based on this technique, a symmetrical turbine is considered below the ground, and the velocity deficits of both the real and image turbines are added, so that the drag conservation is satisfied [4,35]. If this image technique is used to consider the ground effect in Cases (1–5), the normalized velocity deficit differs less than 0.01 at hub height for $x/d < 20$ with respect to a single turbine wake without ground effect. Thus, it seems that the ground has a weak effect on our region of interest, and it is, therefore, neglected in the present research for sake of simplicity.

Another difference between turbine wakes and purely axisymmetric wakes is that the turbine wake rotates in the opposite direction to that of the blades due to conservation of angular momentum [36]. However, experimental [37] and numerical studies [30,33] reported that the wake rotation is weak in the far wake ($x/d > 5$) in the presence of turbulent boundary layer. Hence, its effect is neglected in this study for simplicity.

Next, we investigate the ability of the different analytical wake models to estimate the wind power available for extraction by another turbine placed at a given downwind location, and experiencing full-wake or partial-wake conditions. This available power is denoted as P_{av} and is defined as:

$$P_{av} = \int_{A_0} \frac{1}{2}\rho U_w^3 dA. \quad (22)$$

Therefore, if another turbine is located at that downwind location, it will extract an amount of power from the wind equal to P_{av} multiplied the power coefficient of the turbine C_p, which quantifies the ability of the turbine to extract the energy from the available wind [13]. Fig. 8 shows the available power of the wind passing through a hypothetical turbine rotor located at $x/d = 7$ for different wind directions. In this figure, P_{av} denotes the available power predicted by analytical models, and the one obtained by the LES is denoted by $P_{LES,av}$. The variation of $P_{av}/P_{LES,av}$ versus the wind direction, θ, for the top-hat models reveals that the effect of assuming a top-hat shape for the velocity deficit leads to an inherent error in power prediction with respect to the LES data (see Fig. 8c and d). In fact, if a wind turbine operates in the full-wake of the upwind turbine (i.e., $\theta = 0°$ in Fig. 8), top-hat models typically overestimate its produced power since they underestimate the velocity deficit in these regions. In contrast, if a turbine is located near the edge of the wake (partial-wake conditions), top-hat models underestimate the power due to the overestimation of the velocity deficit (e.g., $\theta = 5°$ in Fig. 8c).

The above discussion therefore leads to the conclusion that top-hat models are adversely sensitive to the relative position of the turbines with respect to the wind direction. For instance, if the wind direction changes only 5° (from $\theta = 0°$ to 5°), $P_{av}/P_{LES,av}$ in Jensen model changes from 15 to 30 percent for the different cases

Please cite this article in press as: Bastankhah M, Porté-Agel F, A new analytical model for wind-turbine wakes, Renewable Energy (2014), http://dx.doi.org/10.1016/j.renene.2014.01.002

(Fig. 8c), and this variation is even more for Frandsen model (Fig. 8d). It is important to note that if these models are used to optimize a wind-farm layout configuration with varying wind directions, this unrealistic behavior of top-hat models can cause considerable errors in the power prediction. By contrast, as shown by Fig. 8b, the difference between the available power predicted by the new proposed model and the one obtained by the LES is much smaller compared with the one obtained with the top-hat models. Furthermore, there is not significant variation in the value of $P_{av}/P_{LES,av}$ as the wind direction changes. It changes only from 3 to 7 percent for the different cases if θ changes from 0° to 5°.

4. Summary

A new analytical model is proposed to predict the deficit of the streamwise velocity in the wake of a wind turbine. To this end, a Gaussian distribution is considered for the velocity deficit in the wake, and mass and momentum conservations are applied to evaluate the velocity profiles downwind of the turbine. Finally, the velocity deficit in the wake can be computed as:

$$\frac{\Delta U}{U_\infty} = \left(1 - \sqrt{1 - \frac{C_T}{8\left(k^* x/d_0 + 0.2\sqrt{\beta}\right)^2}}\right) \times \exp\left(-\frac{1}{2\left(k^* x/d_0 + 0.2\sqrt{\beta}\right)^2}\left\{\left(\frac{z - z_h}{d_0}\right)^2 + \left(\frac{y}{d_0}\right)^2\right\}\right), \tag{23}$$

where β is obtained by Eq. (6) and k^* represents the wake growth rate. In order to predict the wake velocity distribution by the above equation, we only need to specify one parameter (value of k^*) for each case.

The comparison with the high-resolution wind-tunnel measurements [19] and the LES data [33,31] shows that the velocity profiles obtained with the proposed model are in acceptable agreement with the experimental and LES data for 5 different case studies including miniature and real-scale wind turbines with different boundary-layer turbulence conditions. By contrast, the top-hat models, as expected, generally underestimate the velocity deficit at the center of the wake and overestimate it near the edge of the wake. Our results also reveal that the new proposed model is consistent and acceptably accurate in terms of power estimation whereas top-hat models are less accurate and adversely sensitive to the relative position of turbines with respect to the wind direction.

Future research will consider the effect of inflow conditions such as incoming velocity profile and ambient turbulence intensity on the wake expansion parameter, k^*. For this purpose, different experimental and numerical datasets obtained for a range of surface cover types and atmospheric stabilities will be used. In addition, the proposed analytical model will be extended to evaluate velocity profiles inside wind farms for different farm layout configurations and inflow conditions.

Acknowledgments

This research was supported by the Swiss National Science Foundation (grant 200021-132122).

References

[1] Vermeer L, Sørensen J, Crespo A. Wind turbine wake aerodynamics. Prog Aerosp Sci 2003;39:467–510.
[2] Barthelmie RJ, Hansen K, Frandsen ST, Rathmann O, Schepers JG, Schlez W, et al. Modelling and measuring flow and wind turbine wakes in large wind farms offshore. Wind Energy 2009;12:431–44.
[3] Porté-Agel F, Wu YT, Chen C-H. A numerical study of the effects of wind direction on turbine wakes and power losses in a large wind farm. Energies 2013;6(10):5297–313.
[4] Crespo A, Hernandez J, Frandsen ST. Survey of modelling methods for wind turbine wakes and wind farms. Wind Energy 1999;2:1–24.
[5] Katić I, Højstrup J, Jensen N. A simple model for cluster efficiency. In: Proceedings of the European wind energy association conference and exhibition, Rome, Italy 1986. pp. 407–9.
[6] Kiranoudis CT, Maroulis ZB. Effective short-cut modelling of wind park efficiency. Renew Energy 1997;11:439–57.
[7] Frandsen ST. On the wind speed reduction in the center of large clusters of wind turbines. J Wind Eng Ind Aerodyn 1992;39:251–6.
[8] Jensen N. A note on wind turbine interaction. Technical report Ris-M-2411. Roskilde, Denmark: Risø National Laboratory; 1983.
[9] Barthelmie RJ, Folkerts L, Larsen GC, Rados K, Pryor SC, Frandsen ST, et al. Comparison of wake model simulations with offshore wind turbine wake profiles measured by sodar. J Atmospheric Ocean Technol 2005;23:881–901.
[10] Barthelmie RJ, Jensen LE. Evaluation of wind farm efficiency and wind turbine wakes at the nysted offshore wind farm. Wind Energy 2010;13:573–86.
[11] Cleve J, Greiner M, Enevoldsen P, Birkemose B, Jensen L. Model-based analysis of wake-flow data in the nysted offshore wind farm. Wind Energy 2009;12:125–35.
[12] Barthelmie RJ, Frandsen ST, Nielsen MN, Pryor SC, Rethore PE, Jørgensen HE. Modelling and measurements of power losses and turbulence intensity in wind turbine wakes at Middelgrunden offshore wind farm. Wind Energy 2007;10:517–28.
[13] Burton T, Sharpe D, Jenkins N, Bossanyi E. Wind energy handbook. 1st ed. Wiley; 1995.
[14] Marmidis G, Lazarou S, Pyrgioti E. Optimal placement of wind turbines in a wind park using Monte Carlo simulation. Renew Energy 2008;33:1455–60.
[15] Thøgersen ML. Wind PRO/PARK: introduction to wind turbine wake modelling and wake generated turbulence. Technical report. Niels Jernes Vej 10, DK-9220 Aalborg, Denmark: EMD International A/S; 2005.
[16] Crastoa G, Gravdahla A, Castellanib F, Piccionib E. Wake modeling with the actuator disc concept. Energy Procedia 2012;24:385–92.
[17] GH WindFarmer theory manual. Garrad Hassan and Partners Ltd; 2009.
[18] version 1.3 ed. Openwind theoretical basis and validation. AWS Truepower, LCC; 2010
[19] Chamorro LP, Porté-Agel F. Effects of thermal stability and incoming boundary-layer flow characteristics on wind-turbine wakes: a wind-tunnel study. Bound-Layer Meteorol 2010;136:515–33.
[20] Gaumond M, Réthoré PE, Ott S, Peña A, Bechmann A, Hansen KS. Evaluation of the wind direction uncertainty and its impact on wake modeling at the horns rev offshore wind farm. Wind Energy 2013. http://dx.doi.org/10.1002/we.1625.
[21] Frandsen ST, Barthelmie RJ, Pryor S, Rathmann O, Larsen S, Højstrup J, et al. Analytical modelling of wind speed deficit in large offshore wind farms. Wind Energy 2006;9:39–53.
[22] Tennekes H, Lumley JL. A first course in turbulence. The MIT Press; 1972.
[23] Johansson P, George W, Gourlay M. Equilibrium similarity, effects of initial conditions and local Reynolds number on the axisymmetric wake. Phys Fluids 2003;15(3):603–17.
[24] Dufresne N, Wosnik M. Velocity deficit and swirl in the turbulent wake of a wind turbine. Mar Technol Soc J 2013;47(4):193–205.
[25] Chamorro LP, Porté-Agel F. A wind-tunnel investigation of wind-turbine wakes: boundary-layer turbulence effects. Bound-Layer Meteorol 2009;132:129–49.
[26] Troldborg N, Sørensen J, Mikkelsen R. Actuator line simulation of wake of wind turbine operating in turbulent inflow. In: Journal of physics: conference series, vol. 75. IOP Publishing; 2007. p. 012063.
[27] Medici D, Alfredsson P. Measurement on a wind turbine wake: 3d effects and bluff body vortex shedding. Wind Energy 2006;9:219–36.
[28] Markfort CD, Zhang W, Porté-Agel F. Turbulent flow and scalar transport through and over aligned and staggered wind farms. J Turbul 2012;13:1–36.
[29] Zhang W, Markfort CD, Porté-Agel F. Wind-turbine wakes in a convective boundary layer: a wind-tunnel study. Bound-Layer Meteorol 2013;146:161–79.
[30] Porté-Agel F, Wu YT, Lu H, Conzemius RJ. Large-eddy simulation of atmospheric boundary layer flow through wind turbines and wind farms. J Wind Eng Ind Aerodyn 2011;99:154–68.
[31] Wu YT, Porté-Agel F. Atmospheric turbulence effects on wind-turbine wakes: an LES study. Energies 2012;5:5340–62.
[32] Nygaard N, Jensen L, Downey R, Méchali M. Construction and validation of a new offshore wake model. In: ICOWES conference, Lyngby 2013. pp. 26–37.
[33] Wu YT, Porté-Agel F. Large-eddy simulation of wind-turbine wakes: evaluation of turbine parametrisations. Bound-Layer Meteorol 2011;138:345–66.
[34] Pope S. Turbulent flows. Cambridge University Press; 2000.
[35] Lissaman PBS. Energy effectiveness of arbitrary arrays of wind turbines. AIAA 1979;17:8.
[36] Manwell J, McGowan J, Rogers A. Wind energy explained: theory, design and application. Wiley; 2002.
[37] Zhang W, Markfort CD, Porté-Agel F. Near-wake flow structure downwind of a wind turbine in a turbulent boundary layer. Exp Fluids 2012;52:1219–35.

Please cite this article in press as: Bastankhah M, Porté-Agel F, A new analytical model for wind-turbine wakes, Renewable Energy (2014), http://dx.doi.org/10.1016/j.renene.2014.01.002